Contact Geometrical Study for Top Emitting 980 nm InGaAs/GaAsP Vertical-Cavity Surface Emitting Lasers

Faten A. Chaqmaqchee

Department of Physics, Faculty of Science and Health, Koya University, Koya KOY45, Kurdistan Region - F.R. Iraq

Abstract—**Geometrical contacts of a double mesa structure with a 16 rows × 15 columns arrays of top emitting GaAs-based 980 nm vertical-cavity surface emitting lasers (VCSELs) are fabricated and characterized. In this paper, five strained $In_{0.22}Ga_{0.78}As/Ga_{0.9}AsP_{0.1}$ quantum wells within $\lambda/2$ thick cavity have been employed. The top and the bottom epitaxially grown mirrors are based on the linear graded $Al_{0.9}Ga_{0.1}As/GaAs$ distributed Bragg reflectors with 20.5 and 37 periods, respectively. Static parameters including threshold currents, rollover currents, maximum optical output power, and wall-plug efficiency are extracted from light out power-current-voltage (*LIV*) of VCSELs with fixed oxide aperture diameter of $\varnothing\sim 6\ \mu m$ and various mesa2 diameters. In addition, spectral emission for 980 nm VCSELs of oxide aperture between $\varnothing\sim 6$ and 19 μm and with fixed $\varnothing\sim 6\ \mu m$ and different bias currents are analyzed. The highest optical output power of around 33 dBm is observed at bias current of 0.8 mA for short-reach optical interconnect applications.**

Index Terms—**Vertical-cavity surface emitting laser; AlGaAs Distributed Bragg reflectors; InGaAs/GaAsP quantum wells; Static characterization.**

1. Introduction

Today, thousands of optical interconnects (OIs) based on oxide-confined vertical-cavity surface emitting lasers (VCSELs) and multimode fibers (MMFs) are generally mounted in high-performance computers (Choquette, et al., 1994). VCSELs at 980 nm have recognized as key components in short-reach MMF applications and dominantly deployed in OIs in datacenters, supercomputers, and data storage systems to meet requirements of high modulation bandwidth and energy efficiency (Taubenblatt, 2011; DeCusatis, 2013; Haghighi and Lott, 2021). VCSELs are semiconductor lasers with unique geometry of low threshold current, low divergent angle, and circular beam that reduce electrical power conversion and emitted single longitudinal mode at desired wavelengths (Iga, 2000; Chaqmaqchee, 2020). The design of the VCSEL structure can achieve low resistance distributed Bragg mirrors

(distributed Bragg reflectors [DBRs]) and low optical loss by optimization of doping concentration of top mirrors. When the oxide layer has larger aperture diameters, it reduces the capacitance. When the aperture is small, it slows down the laser speed (Castro, et al., 2015). However, VCSELs have higher electrical resistance due to their small top contact area and high resistive of DBRs mirrors (Chaqmaqchee, 2021). The contact geometry of the two-mesa VCSEL allows a combination of low electrical parasitics and high thermal conductivity of VCSELs (Ou, et al., 2009; Mutig and Bimberg, 2011). VCSELs at short emission wavelengths are formed from compressively strained InGaAs quantum wells (QWs) lattice matched to GaAs and surrounded by GaAs, AlGaAs, or GaAsP barrier layers to achieve high differential gain (Healy, et al., 2010). VCSELs have been motivated by the market demand, as a result of demonstrating of VCSELs at high modulation bandwidth (Blokhin, et al., 2009; Haghighi, et al., 2020) and possibility with the highest wall-plug efficiency (WPE) to help dissipate heat and to help lower series resistance (Haghighi, et al., 2020).

In this study, we have focused on a geometrical study of 980 nm VCSEL at various top mesa diameters. The sizes of double mesa high-speed VCSELs are arranged in a 16 rows × 15 columns arrays. Static characteristics with different top mesa diameters give information on VCSELs performance, including threshold currents, maximum output powers, and rollover currents that extracted from the light output power-current-voltage (*LIV*) and WPE. In addition, optical emission spectra measurements were measured at fixed column of B and at row diameters from 0 to F. VCSELs with aperture diameter of $\varnothing\sim 6\ \mu m$ at 25°C were designed to reduce the order modes with the current confinement profile. Low threshold current of ~ 0.5 mA with top mesa diameter of 18 μm was achieved for almost all the diameters of rows 0, 9, B, D, and E. Maximum WPE of 12% with top mesa diameter of 26 μm and diameters of rows B and maximum output power of 33 dBm at bias current of 0.8 mA for fixed column of B and at row diameters of 0 were obtained.

II. Materials and Method

In this study, the epitaxial structure of VCSEL was grown on a semi-insulating of 1.5857 μm thick (n+) GaAs (100) substrate by metal-organic chemical vapor deposition and

designed to emit at wavelength of 980 nm (Chaqmaqchee and Lott, 2020). To reduce the device capacitance, two oxide layers, a thick layer of benzocyclobutene (BCB), are used under the p-bond pad and an undoped substrate (Lau and Yariv, 1985; Hofmann, 2010). VCSELs at 980 nm require a lower drive voltage and are possible to design with deeper and more strained QWs that improve differential gain and thus the intrinsic and thermally limited bandwidths (Chaqmaqchee, 2020). Resistance and optical loss in the DBRs are minimized using modulation doping and graded interfaces, and thermal impedance is lowered using binary alloys in DBR, which all ease operation at high temperatures (Moser, et al., 2014). Fig. 1(a) depicts the schematic cross-section of the 980 nm VCSEL structure. VCSELs were fabricated through standard processing techniques including optical lithography, dry etching, wet oxidation, and metal contact deposition. Reactive ion etching is applied to form top and bottom DBRs mesas. VCSELs show single mode and multimode behaviors with smaller and larger aperture diameters, respectively. Two 20 nm thick $Al_{0.98}Ga_{0.02}As$ layers are separated by half wavelength to increase the optical confinement factor and reduce the carrier transport times (Nagarajan, et al., 1992; Westbergh, et al., 2012). The double oxide apertures are placed as close to the QWs as possible to confine the current and the optical fields, and it is formed by high selectivity of wet oxidation with controlled oxidation furnace. Active region includes five strained $In_{0.22}Ga_{0.78}As/Ga_{0.9}AsP_{0.1}$ QWs for high differential gain. The top mirror consists of 20.5 pairs p-doped $Al_{0.9}Ga_{0.1}As/GaAs$ DBRs and 37 pairs n-doped $Al_{0.9}Ga_{0.1}As/GaAs$ top mirrors.

The VCSELs have a double mesa structure and uniformly distributed with a 16 rows ×15 columns arrays. The top mesa diameters are varied from 18 μm in row 0 to 31 μm in row F, whereas the bottom mesa diameters is varied from 0 in column 0 to 60 μm in column E. The VCSEL set is differ in the double mesa design and the geometric design and the position of the bottom contact. Fabrication procedure begins with etching of top mesas surface and then selectively oxidized to form 6 μm diameter apertures. A cathode contact is formed by etching a bottom mesa to the b-contact layer. Finally, the structure is planarized with bis(benzocyclobutane) (BCB) and deposited with bond pads. Fig. 1(b) shows part of an optical microscope image of the fabricated VCSEL array together with a zoomed view of a VCSEL with the unit cell of 33 and the top mesa diameter of 22 μm (with fixed column of 4 and variable row of 6). Devices that fabricated with small aperture diameters exhibited stable bandwidths than bigger aperture diameter at room temperature.

The static characteristics output light-current-voltage (*LIV*) is automatically determined and evaluated using homemade mapping system. The output light from the VCSEL is coupled into a MMF connected using an optical spectrum analyzer Ando model AQ6317C to analyze the optical emission spectra over ~780–1180 nm, where the VCSELs are driven by the digital source meter Keithley model 2400-LV and the measurements are controlled by LabVIEW program running on a Microsoft Window-based personal tower computer.

III. Results and Discussion

We performed static optical output power-current-voltage (*LIV*) and optical spectral emission for VCSELs at room temperature with different mesa and fixed oxide aperture diameter of 6 μm showed various threshold current, rollover current, and output powers. Fig. 2 shows the threshold current versus top mesa diameters between 18 and 31 μm. With increasing mesa diameters, the threshold current increased linearly from 18 to 31 μm, where the diameters are almost constant for 18 μm diameters of row E, D, B, 9, and 0, whereas the diameters are between 1.89 for row 0 and 8.58 of row E of 31 μm diameters. The lowest threshold currents were recorded between 0.48 and 1.89 μm in row 0 for 31 μm diameter. Fig. 3 presents maximum output power of VCSELs with different diameter and fixed oxides aperture diameter. The output power increased linearly as a result of increasing the top mesa diameters from 18 μm (P_{out} Max. from 0.47 of row 9 to 0.86 mW of row D) to 31 μm (P_{out} Max. from 2.98 of row E to 5.98 mW of row B). In addition, the maximum current (*I*) point is extracted from the light output power-current (*LI*) rollover for various mesa diameters. Fig. 4 illustrates the maximum rollover currents of VCSELs that varied for top mesa diameter from 18 to 31 μm between 9.70 mA to 26.55 mA of row 9 and between 14.72 and 32.95 mA for row 0.

In addition, WPE as a function of top mesa diameters is depicted in Fig. 5. LabVIEW program was used to swept the
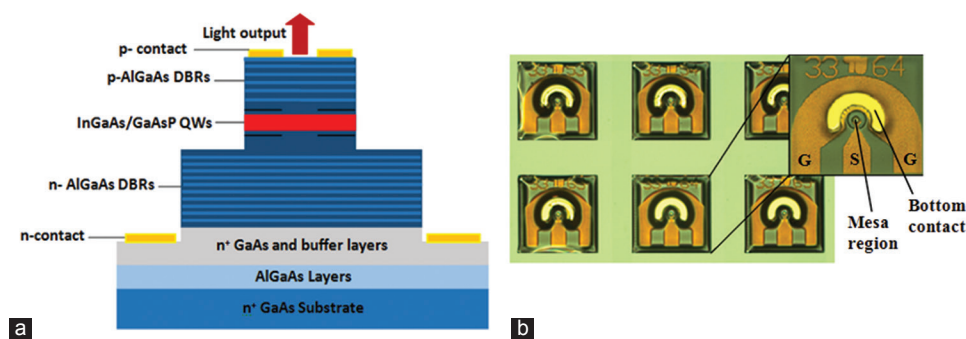
Fig. 1. (a) Schematic cross-section of 980 nm GaAs-based vertical-cavity surface emitting lasers (VCSELs) features an active region sandwiched between top and bottom DBRs mirrors, (b) optical microscope image of the fabricated array of VCSELs including an expanded top-down view of a device.
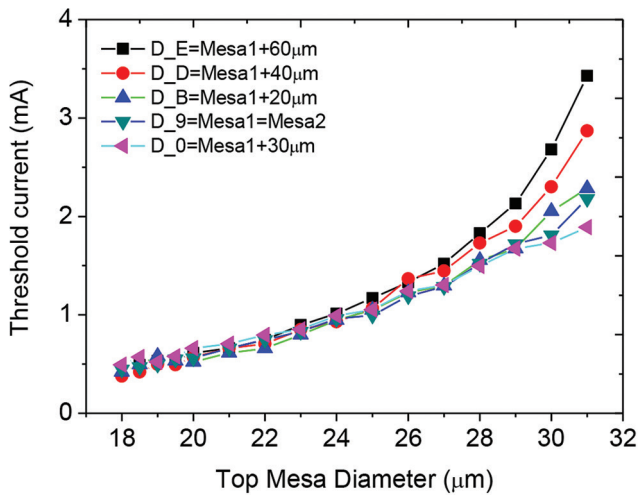
Fig. 2. Threshold current versus top mesa diameter for vertical-cavity surface emitting lasers diameters of rows 0, 9, B, D, and E.
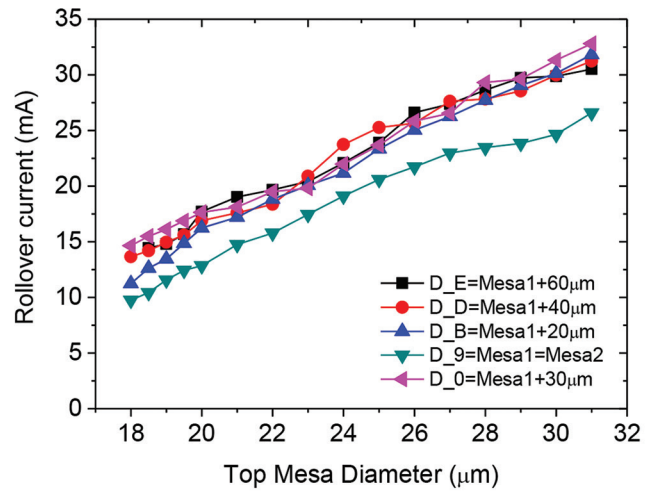
Fig. 4. Rollover current versus top mesa diameter for vertical-cavity surface emitting lasers diameters of rows 0, 9, B, D, and E.
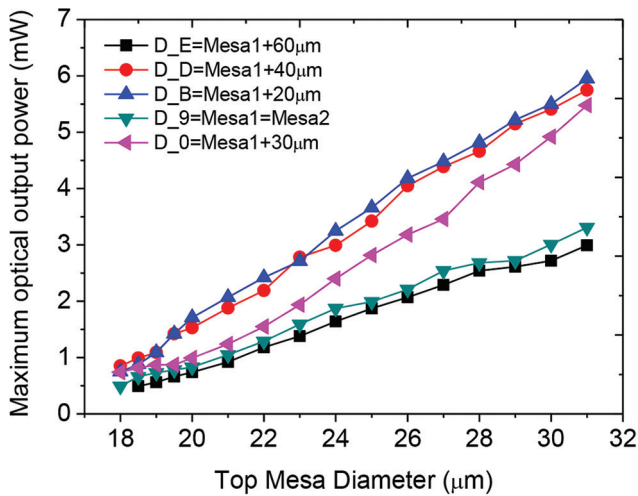
Fig. 3. Maximum output power versus top mesa diameter for vertical-cavity surface emitting lasers diameters of rows 0, 9, B, D, and E.
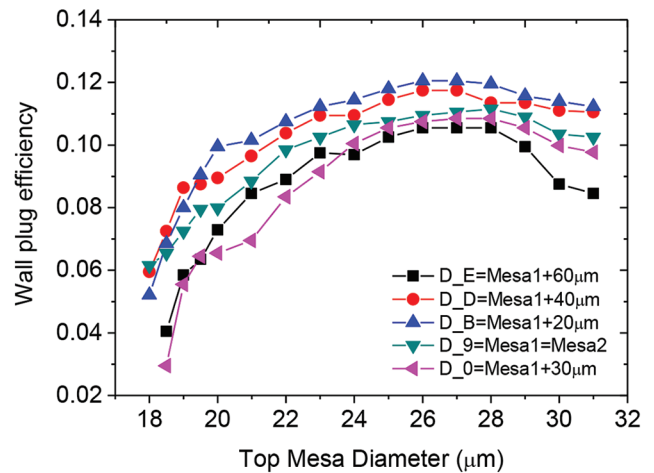
Fig. 5. Wall-plug efficiency versus top mesa diameter with vertical-cavity surface emitting lasers diameters of rows 0, 9, B, D, and E at 25°C.

bias current (I) with a Keithley 2400-LV and measuring the static light output power (L), current (*I*), and voltage (V). The WPE (WPE = $100 \times L/(I \times V)$ as a percentage) versus top mesa diameters were extracted from the maximum value of WPE with current increasing then decreases with increasing current for different Rows. The WPE is bended as a result of increasing the top mesa diameters from 18 to 26 μm and reaches maximum values of 0.12 in row B and 0.10 in row E. Thus, a large WPE allows more power to convert into potentially useful optical power (Choquette, et al., 1997).

The optical spectra at fixed column of B and rows of 0, 1, 2, 3, 4, 5, 6, 7, 8, 9, A, B, C, D, E, and F are shown in Fig. 6. The optical spectrum at temperature of 25°C shows a typical number of around 4 to 10 transverse modes that contribute to the emitted power and the bias current is just above threshold at 1 mA. The device with a smaller aperture diameter has the fewer existed optical mode caused by the small lateral confinement aperture design. Larger aperture diameter generates further modes existed in the VCSEL

due to the weak optical confinement. In Fig. 6a-c, the center wavelength of VCSELs spectra at this bias current is around 980 nm whereas in Fig. 6d, the center wavelength is in the region of 977 nm. When the device has smallest aperture diameter, the spectral width for the single mode is around 0.2 nm for oxide apertures between 6 and 11 μm as in Fig. 6(a) and (b) with an optical power of around 22.7 dBm for $\varnothing \sim 6$ μm, whereas the output power for $\varnothing \sim 6.5$ μm is about 16.81 dBm. However, when the aperture diameter is getting larger, the side mode suppression ratio decreases and thus the spectral width of $\Delta\lambda$ increases which is varied between 1.3 and 2.7 nm as shown in Fig. 6(c) and (d).

The spectrum of the VCSEL emission at below and above threshold currents with VCSEL aperture diameter of $\varnothing \sim 6$ μm is presented in Fig. 7, where two modes are clearly visible at around 980 nm. At higher bias current, the emissions become strongly multimode and a red shift is observed. The number of transverse multiple modes of VCSEL increases when an oxides aperture diameter increases (Satuby and Orenstein, 1999). The peak emission wavelengths at lower bias current
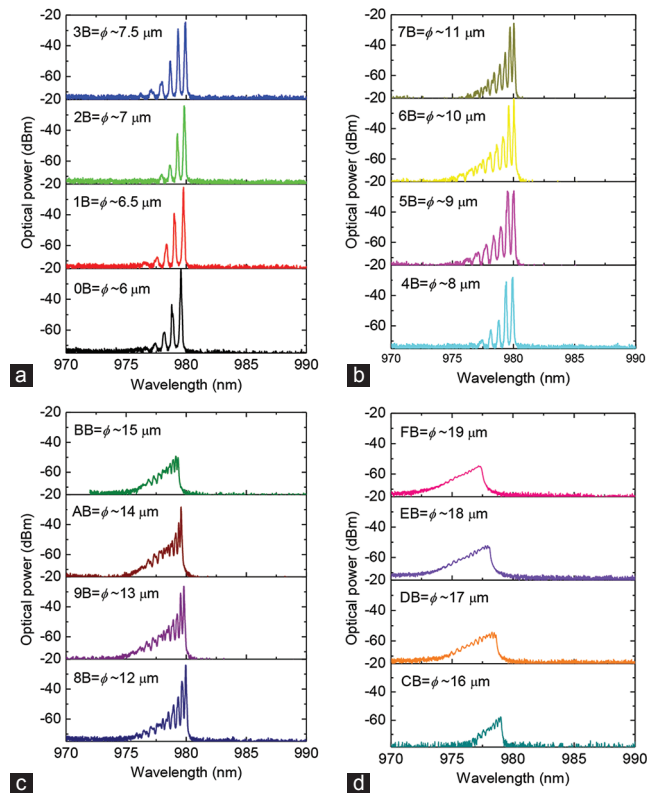
Fig. 6. Spectral emission for a 980 nm vertical-cavity surface emitting lasers with: (a, b) ∅ from 6 to 11 µm and (c, d) ∅ from 12 to 19 µm measured at fixed column of B and at row diameters from 0 to F through bias current of 1 mA at 25°C.
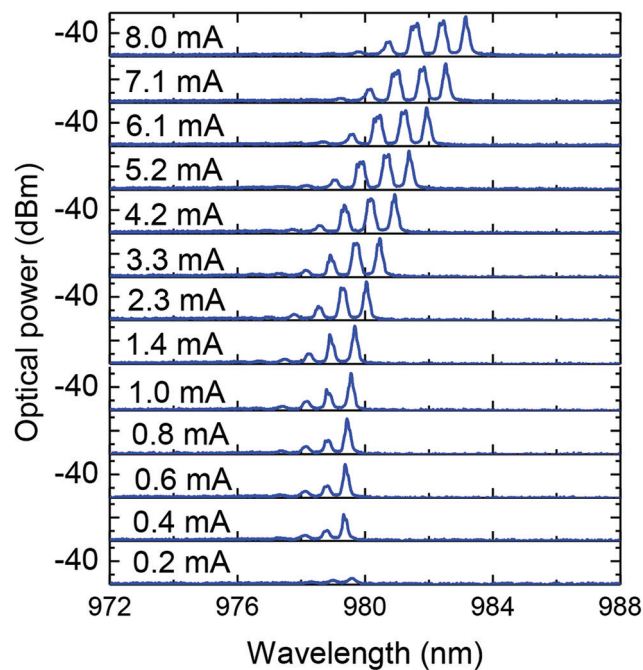
Fig. 7. Optical spectra measurements for vertical-cavity surface emitting lasers of ∅ ~ 6 µm with different bias currents.

of 0.8 mA are about 978.8 and 979.6 nm, the highest optical output power at ~33 dBm at center emission of 979.6 nm is observed. Their spectral emission width is about 0.21 nm

which reduces the chromatic dispersion to send data over longer distances.

IV. Conclusion

The performances of top emitting VCSELs at room temperature have been demonstrated. Geometrical study of two mesa VCSELs with sizes of 16 rows × 15 columns arrays is fabricated and characterized including threshold currents, rollover currents, maximum optical output power' and wall-plug efficiency which are extracted from current-voltage-power of VCSELs with oxide aperture diameter of ∅~ 6 µm and various mesa2 diameters. In addition, spectral emission of oxide aperture between ∅~ 6 and 19 µm and with fixed ∅~ 6 µm and different bias currents are analyzed. At low bias current of 0.8 mA, we obtained high optical power of 33 dBm for small device of □~ 6 µm, which corresponding top mesa diameters of around 18 µm. This wavelength is suitable for future short reach OIs, particularly in high-performance computers (HPC) applications. Throughout the increasing demand for VCSELs in markets, companies and research institutions are following the development of research, optimizing VCSEL performance, and improving output power in the near future.

V. Acknowledgment

References

Blokhin, S., Lott, J.A., Mutig, A., Fiol, G., Lederntsov, N.N., Maximov, M.V., Nadtochiy, A.M., Shchukin, V.A. and Bimberg, D., 2009. Oxide-confined 850 nm VCSELs operating at bit rates up to 40 Gbit/s. *Electronics Letters*, 45(10), pp.501-503.

Castro, J.M., Pimpinella, R., Kose, B., Huang, Y., Lane, B., Szczerba, K., Westbergh, P., Lengyel, T., Gustavsson, J.S., Larsson, A. and Andrekson, P.A., 2015. 48.7-Gb/s 4-PAM transmission over 200 m of high bandwidth MMF using an 850-nm VCSEL. IEEE Photonics Technology Letters, 27(17), pp.1799-1801.

Chaqmaqchee, F.A., 2020. Long-wavelength GaInNAs/GaAs vertical-cavity surface-emitting laser for communication applications. *Aro-the Scientific Journal of Koya University*, 8(1), pp.107-111.

Chaqmaqchee, F.A., 2021. A comparative study of electrical characterization of p-doped distributed Bragg reflectors mirrors for 1300 nm vertical cavity semiconductor optical amplifiers, *Aro-The Scientific Journal of Koya University*, 9(1), pp.89-94.

Chaqmaqchee, F.A.I. and Lott, J.A., 2020. Impact of oxide aperture diameter on optical output power, spectral emission, and bandwidth for 980 nm VCSELs. *OSA Continuum*, 3(9), pp.2602-2613.

Chaqmaqchee, F.A.I., 2020. Gain analysis of vertical-cavity surface-emitting laser for long optical fiber communication. *Journal of Optoelectronics and Advanced Materials*, 22(7-8), pp.339-343.

Choquette, K., Schneider, R.P., Lear, K.L. and Geib, K.M., 1994. Low threshold

voltage vertical-cavity lasers fabricated by selective oxidation. *Electronics Letters*, 30(24), pp.2043-2044.

Choquette, K.D., Chow, W.W., Hadley, G.R., Hou, H.Q. and Geib, K.M., 1997. Scalability of small-aperture selectively oxidized vertical cavity lasers. *Applied Physics Letters*, 70(7), pp.823-825.

DeCusatis, C., 2013. Optical interconnect networks for data communications. *Journal of Lightwave Technology*, 32(4), pp.544-552.

Haghighi, N. and Lott, J.A., 2021. Electrically parallel three-element 980 nm VCSEL arrays with ternary and binary bottom DBR mirror layers. *Materials*, 14(2), pp.1-17.

Haghighi, N., Moser, P. and Lott, J.A., 2020. 40 Gbps with electrically parallel triple and septuple 980 nm VCSEL arrays. *Journal of Lightwave Technology*, 38(13), pp.3387-3394.

Haghighi, N., Moser, P., Zorn, M. and Lott, J.A., 2020. 19-element vertical cavity surface emitting laser arrays with inter-vertical cavity surface emitting laser ridge connectors. *Journal of Physics: Photonics*, 2(4), pp.04LT01.

Healy, S.B., O'Reilly, E.P., Gustavsson, J.S., Westbergh, P., Haglund, A., Larsson, A. and Joel, A., 2010. Active region design for high-speed 850-nm VCSELs. *IEEE Journal of Quantum Electronics*, 46(4), pp.506-512.

Hofmann, W., 2010. High-speed buried tunnel junction vertical-cavity surface-emitting lasers. *IEEE Photonics Journal*, 2(5), pp.802-815.

Iga, K., 2000. Surface-emitting laser-its birth and generation of new optoelectronics filed. *IEEE Journal of Selected Topics in Quantum Electronics*, 6(6), pp.1201-1215.

Lau, K. and Yariv, A., 1985. Ultra-high speed semiconductor lasers. *IEEE Journal of Quantum Electronics*, 21(2), pp.121-138.

Moser, P., Lott, J.A., Wolf, P., Larisch, G., Li, H. and Bimberg, D., 2014. Error-free 46 Gbit/s operation of oxide-confined 980 nm VCSELs at 85 C. *Electronics Letters*, 50(19), pp.1369-1371.

Mutig, A. and Bimberg, D., 2011. Progress on high-speed 980nm VCSELs for short-reach optical interconnects. *Advances in Optical Technologies*, 2011, pp.1-15.

Nagarajan, R., Ishikawa, M., Fukushima, T., Geels, R.S. and Bowers, J.E., 1992. High speed quantum-well lasers and carrier transport effects. *IEEE Journal of Quantum Electronics*, 28(10), pp.1990-2008.

Ou, Y., Gustavsson, J.S., Westbergh, P., Haglund, A., Larsson, A. and Joel, A., 2009. Impedance characteristics and parasitic speed limitations of high-speed 850-nm VCSELs. *IEEE Photonics Technology Letters*, 21(24), pp.1840-1842.

Satuby, Y. and Orenstein, M., 1999. Mode-coupling effects on the small signal modulation of multi transverse-mode vertical-cavity semiconductor lasers. *IEEE Journal of Quantum Electronics*, 35(6), pp.944-954.

Taubenblatt, M.A., 2011. Optical interconnects for high-performance computing. *Journal of Lightwave Technology*, 30(4), pp.448-457.

Westbergh, P., Safaisini, R., Haglund, E, Kögel, B. Gustavsson, J.S., Larsson, A., Geen, M., Lawrence, R. and Joel, A., 2012. High-speed 850 nm VCSELs with 28 GHz modulation bandwidth operating error-free up to 44 Gbit/s. *Electronics Letters*, 48(18), pp.1145-1147.